Acta Cryst. (1975). A31, 273

Removal of the White-Radiation Background from Data Collected with β-Filtered Mo *Kα* and Ag *Kα* X-rays

BY R. J. NELMES

Department of Physics, University of Edinburgh, Mayfield Road, Edinburgh EH9 3JZ, Scotland

(*Received* 1 *July* 1974; *accepted* 18 *November* 1974)

The usual methods of collecting diffraction data using β-filtered X-rays lead to significant systematic errors in the low-angle data, especially when the shorter-wavelength radiations (*e.g.* Mo *Kα* and Ag *Kα*) are employed. These errors arise because of the structure introduced into the white-radiation background by the filter absorption edge. A technique is proposed for the correct removal of the structured white-radiation profile from low-angle data. Some experimental measures are recommended which will reduce the number of reflexions affected. The proposed procedures are simple and can be carried out 'by hand' or, preferably, incorporated in the data-reduction program. Given an accurate and easily applied technique for removing the white-radiation background, it is argued that in the majority of cases data collection with β-filtered radiation is to be preferred over other methods such as the use of monochromated radiation or balanced filters.

1. Introduction

For some time those in search of very accurate X-ray data have used monochromator or balanced-filter techniques to remove the white-radiation background. The conditions for the successful application of these methods are stringent [see Coppens, Ross, Blessing, Cooper, Larsen, Leipoldt, Rees & Leonard (1974) p. 318], and often the time, equipment and effort needed either are not available or are inconsistent with the (lower) accuracy of data actually required: the uncritical use of a monochromator or balanced filters will, in any case, yield relatively poor results. For such reasons it is still both common and good practice to collect X-ray data, whether on a diffractometer or with film, with β-filtered radiation.

In the β-filter method the white-radiation background is usually removed by a linear truncation between background measurements made on the low-angle and high-angle sides of the characteristic peak. For normal H.T. settings (40–50 kV) this procedure leads to serious errors in the integrated intensities so obtained from data collected with the shorter wavelengths (*e.g.* Mo *Kα* and Ag *Kα*) in the low θ(Bragg) range. These errors arise when the sharply structured part of the white-radiation spectrum introduced by the filter absorption edge is Bragg-reflected close to, or even (at very low θ) within, the instrumental width of the characteristic peak. The problem can be avoided in diffractometer data collection by removing the filter for the low-θ range: but this introduces uncertainties, such as scaling, and may be impracticable. Such a solution is yet less feasible with film techniques. Attention has been drawn to the difficulty before (Alexander & Smith, 1962; Young, 1965; Kheiker, 1969) but no solution proposed other than removal of the β filter or recourse to balanced filters – except that Young (1965) suggested a procedure that amounts to a rough approximation to the methods developed in this paper.

It is the purpose of this paper to show that the structured white-radiation background can be removed from β-filter data correctly by simple extensions of the normal methods of data collection and data reduction. The full use of $\omega/2\theta$ diffractometer step scans (or the equivalent on film) extends to lower θ the range over which the background–background truncation *can* be used; and a procedure is proposed for the lowest θ range – in which the absorption-edge structure is 'under' the characteristic peak. Examples are taken from $\omega/2\theta$ four-circle diffractometer step scans – to which the specific form of the procedures given here is applicable. In principle film data can be treated in an equivalent way.

Other contributions to background structure – such as thermal diffuse scattering – are not considered. They can, in general, be treated independently of the problem on which attention is focused here.

In this paper it is convenient to introduce a distinction between the overall angular variable of Bragg reflexion, θ, (with limits $0° \le \theta \le 90°$), and the variation of θ within the range of a particular reflexion. The latter will be denoted by ω. For the various components of an observable reflexion profile ω dependence is not explicitly stated, but θ dependence is, *e.g.* $I_0(\theta)$.

2. The background structure

The spectrum emitted by a molybdenum (Mo) tube operating at an H.T. of 50 kV, as reflected by an analysing crystal, is shown in Fig. 1(*a*) of Ladell & Spielberg (1966). The effect of introducing a zirconium (Zr) filter and pulse-height analysis is shown in their Fig. 1(*b*). The essential features of these figures are reproduced here in Fig. 1(*a*) and Fig. 1(*b*) respectively. For

a silver (Ag) tube with a palladium (Pd) filter the spectra are essentially the same, but the characteristic lines are at a lower wavelength ($\lambda_{K\bar{\alpha}}=0{\cdot}56$ Å) and thus, for a given H.T., nearer to the white-radiation peak.

In data collection with β-filtered radiation, the observable reflexion profile, $I_0(\theta)$, is the convolution of the spectral function incident on the specimen crystal [Fig. 1(*b*)] with (i) the intrinsic diffraction pattern, (ii) the source intensity distribution, (iii) the crystal size and shape, and (iv) the crystal mosaic spread (see Ladell & Spielberg, 1966). It will be assumed that the spectral function can be represented adequately by a simple white-radiation profile, $I_b(\theta)$, together with the characteristic $K\alpha$ line, I_c, which is taken to be a single δ function [Fig. 2(*a*)]. The residual $K\beta$ line [Fig. 1(*b*)] is not negligible but it is irrelevant to the present considerations. The α_1/α_2 splitting of the $K\alpha$ line is very small in the low θ range (but see below). The smearing introduced by factors (i), (ii), (iii) and (iv) above will be represented by a resolution function, R [Fig. 2(*b*)]. It is assumed that in any particular experiment R is given by the observed peak shape as $\theta \rightarrow 0°$. Thus, in practice, R includes the finite but negligibly small spectral line width. The θ-dependent effects included in R are small compared with the spread introduced by specimen and source size, and for simplicity of presentation R will be assumed to be constant (in shape) over the θ range considered. The small spread of R with increasing θ that occurs in practice matters only to the extent that the range of the characteristic peak profile increases slightly. The principal reason for increase in the characteristic peak width with increasing θ is the α_1/α_2 splitting. This also introduces no essential difficulty, and is neglected in the presentation. The observable reflexion profile includes the general background scatter, I_g. This is assumed to vary only linearly with ω. Structured background scatter, arising, for example, from a powder line of the glass fibre supporting the specimen, will not be considered. Such problems do not present any especial difficulties if a complete step-scan is recorded and inspected.

The components of the observable reflexion profile, $I_0(\theta)$, are then

$$I_0(\theta)=I_g+R*I_b(\theta)+R*I_c \qquad (1)$$

where $*$ denotes convolution. The θ dependence of the white-radiation spectrum implied by the notation $I_b(\theta)$ arises because the range of ω over which the spectrum is Bragg reflected is a function of θ (see Fig. 4). This is the nub of the problem considered here.

The characteristic peak profile $R*I_c$ will be denoted I_c^R. The experimental objective is to measure the integrated intensity, I, which is the area under the profile I_c^R. A common method of measuring I is (i) to integrate through the expected peak position over a range that is the known peak width, W, plus an amount that allows for mis-setting and misalignment of the specimen, (ii) to measure the background level at positions one to two times W out on each side of the expected peak position, and (iii) to remove the background by a linear interpolation between these background measurements. This will be referred to subsequently as the background–peak–background, or BPB, method. The white-radiation background profile, $R*I_b(\theta)$, is denoted $I_b^R(\theta)$. The convolution of R (taken for this purpose to be Gaussian) with the triangle function of $I_b(\theta)$ leads to an unwieldy expression. But here an adequate approximation for R (see below) is an isosceles triangle of the same 'base width'. The base width, 2ϵ, of R is taken as the angular range over which there is a discernible characteristic peak profile as $\theta \rightarrow 0°$ [see Fig. 2(*b*)], or, more precisely, twice the width at half height of this profile. Before convolution the spectrum $I_b(\theta)$ in Fig. 2(*a*) has to be expressed as a function of θ. In the θ range considered the effect of this transformation on the *form* of $I_b(\theta)$ is insignificant, but the range of ω over which $I_b(\theta)$ is reflected by the specimen varies as $\tan\theta$: *i.e.* $I_b(\theta)$ becomes a triangle function with a θ-dependent base length. At an operating H.T. of 50 kV this length, denoted γ, is approximately 20 $\tan\theta$ degrees for both Mo and Ag radiation. The result of the convolution is shown in Fig. 3 as $I_b^{R'}(\theta)$, an approximation to $I_b^R(\theta)$; and experimentally observed profiles show the approximation to be qualitatively a good one. The low-angle cubic shape

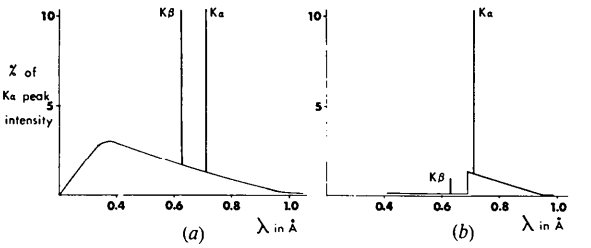

Fig. 1. The essential features of the spectrum emitted from a molybdenum (Mo) tube at 50 kV (after Ladell & Spielberg, 1966), (*a*) without filtration and (*b*) after passing through a Zr filter and pulse-height analysis.

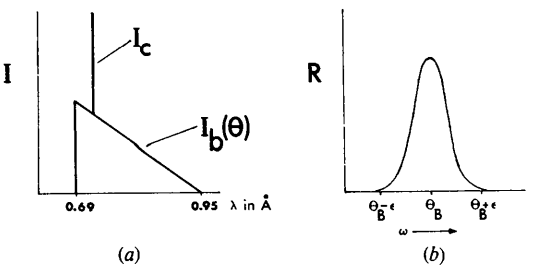

Fig. 2. Components of the observable reflexion profile, $I_0(\theta)$. The incident spectrum is composed of the white radiation, $I_b(\theta)$, and the characteristic line, I_c, shown in (*a*) as functions of wavelength – the values given being for Zr-filtered Mo radiation. This incident spectrum is convoluted with the resolution function, R, shown in (*b*): θ_B is the Bragg reflexion angle for the wavelength reflecting at the peak of R, and ϵ characterizes the angular spread of R.

followed by a linear fall-off is seen in Fig. 5 (*e*, *g*, and *h*). The linear fall-off with the break away approximately at $\gamma-\epsilon$ is seen in Fig. 5(*a*) and in other such cases where a very strong reflexion has only weak (or no) reflexions over this range (*i.e.* up to $\sim\gamma$) on its high-angle side. The features of $I_b^R(\theta)$ which are important here also appear in the convolution with a Gaussian R. They are (see Fig. 3).

(1) that from $-\epsilon$ to ω_p $\partial I_b^R(\theta)/\partial\omega$ increases up to $\omega=0$ and decreases approximately symmetrically up to $\omega=\omega_p$,

(2) that from ω_p the profile is linear, and

(3) that ω_p is not coincident with the point $\omega=\epsilon$, but

(4) that in practice ω_p is close to the point $\omega=\epsilon$.

The more tractable analysis arising from approximating R by a triangle gives as an estimate of ω_p,

$$\omega_p=\gamma+\epsilon-\sqrt{\gamma^2+2\epsilon^2}. \qquad (2)$$

Since under normal conditions ϵ remains much less than γ down to very low angles, ω_P differs from ϵ by a small amount – and its value is thus insensitive to the crude approximation of a triangular R. Over the range of measurement of any reflexion it is assumed that I_g varies slowly and may be taken to be linear. In the low-θ range reflexions are sometimes mounted on the linear part of the white-radiation profile of a strong reflexion occurring at a lower Bragg angle [see, for example, Fig. 5(*b*)]. This contribution to the background can be included in a linearly varying I_g.

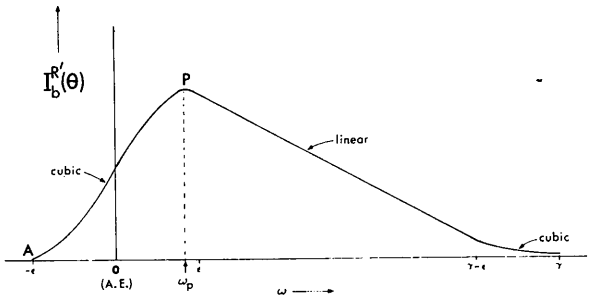

Fig. 3. An approximation to the white-radiation-background profile. The origin, *O*, is taken at the angle at which the filter absorption-edge wavelength is Bragg reflected. The symbols used are explained in the text.

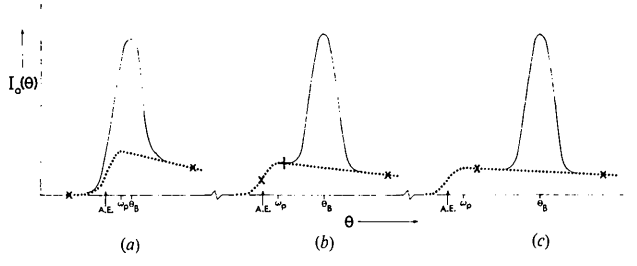

Fig. 4. A diagrammatic representation of 'observed' reflexion profiles at Bragg angles (θ_B) increasing in the order (*a*), (*b*), (*c*). ω_p is the position of the highest point of the white-radiation profile, $I_b^R(\theta)$, which is shown dotted. A.E. is the angle at which the filter absorption-edge wavelength is reflected. The crosses (×) mark the points at which background measurements are made in a typical BPB scan. The cross (+) in (*b*) marks the point at which the low-angle background is measured in the βPB method. I_g is not included.

Fig. 4 illustrates the changing form of the observed profile, $I_0(\theta)$, as θ increases in the order (*a*), (*b*), (*c*). The general background, I_g, has been omitted. Within the given assumptions the characteristic peak width remains unaltered, but the ω range of $I_b^R(\theta)$ diminishes with θ. Thus, if the BPB method is used with the background measurements made at the positions marked ×, the simple truncation procedure is adequate for (*c*) but not for (*a*) or (*b*). In the case of (*b*) linear truncation is possible if the low-angle background measurements are made at +. In (*a*) measurements of $I_b^R(\theta)$ can be made *only on the high-angle side of the characteristic peak.*

It is evident that failure to recognize the situations shown in Figs. 4(*a*) and 4(*b*) will lead to an overestimation of the integrated intensity. The error introduced by applying the BPB method can be considerable – errors of up to 15% on I for Zr-filtered Mo $K\alpha$ and up to 100% on I for Pd-filtered Ag $K\alpha$ have been encountered. Some examples of observed profiles measured with Mo $K\alpha$ (Zr-filtered) and Ag $K\alpha$ (Pd-filtered) are reproduced in Fig. 5. The principal difference between the two radiations is that, for a given operating H.T., the Pd-filtered Ag radiation has a higher proportion of white radiation in the incident spectrum (see Fig. 5). This arises partly from reduced $K\alpha$ intensity and partly from the characteristic line being nearer the peak of the white radiation – in Fig. 1(*a*) the white radiation profile will be similar but the $K\alpha$ line is at $\lambda=0{\cdot}56$ Å. [For Ni-filtered Cu radiation at a normal working H.T. – 30 to 50 kV – the characteristic wavelength is large enough to be well separated from the peak of the white radiation, and the errors discussed in this paper become negligibly small.]

Hereafter 'low-θ range' will be taken to denote the range of θ in which an automatic data collection procedure (*e.g.* BPB) cannot with reasonable certainty make background measurements on the linear part of $I_b^R(\theta)$ on *both* sides of I_c^R – so that the situations shown in Figs. 4(*a*) and 4(*b*) occur.

3. Removal of the white-radiation background

The object, then, is to find the integrated intensity under I_c^R by removing $I_g+I_b^R(\theta)$ from the observed $I_0(\theta)$. With regard to the white-radiation profile, $I_b^R(\theta)$, three cases have been distinguished in Fig. 4. In (*c*) the BPB method is adequate on the assumption that the setting and alignment are good enough to keep the low-angle background measurement above ω_p. In (*b*) the low-angle background estimation must be made at a position between ω_p and the extremity of the characteristic peak, I_c^R. In (*a*) the form of $I_b^R(\theta)$ has to be

constructed from measurements of its linear part made on the high-angle side only.

Certain experimental requirements are imposed. The observed profile must be measured along a radial direction in reciprocal space: for equatorial four-circle geometry this means using the $\omega/2\theta$ scan. Even in case (*c*) any technique that fails to distinguish the white-radiation profile, $I_b^R(\theta)$, will give a poor estimate of the background. Furthermore, in (*a*) and (*b*) the individual measurements of a step scan are needed. For (*b*) this is a practical requirement: it is assumed [in defining (*b*)] that the experimental conditions are not well enough known or stabilized for measurements between ω_p and I_c^R to be made under automatic control – yet, so long as ω_p and I_c^R are separated, the one or more step-scan measurements made between them will give an estimate of the background as good as or better than the procedure to be adopted in case (*a*). The determination of the correct low-angle background in this way will be referred to as the βPB method – a modified form of BPB. For (*a*) the individual measurements are required (i) to characterize the linear part of the $I_b^R(\theta)$ profile and (ii) to locate accurately the relative positions of features in a structured profile. In passing it is emphasized that recording and inspecting the complete step scan is desirable in any case, as a general

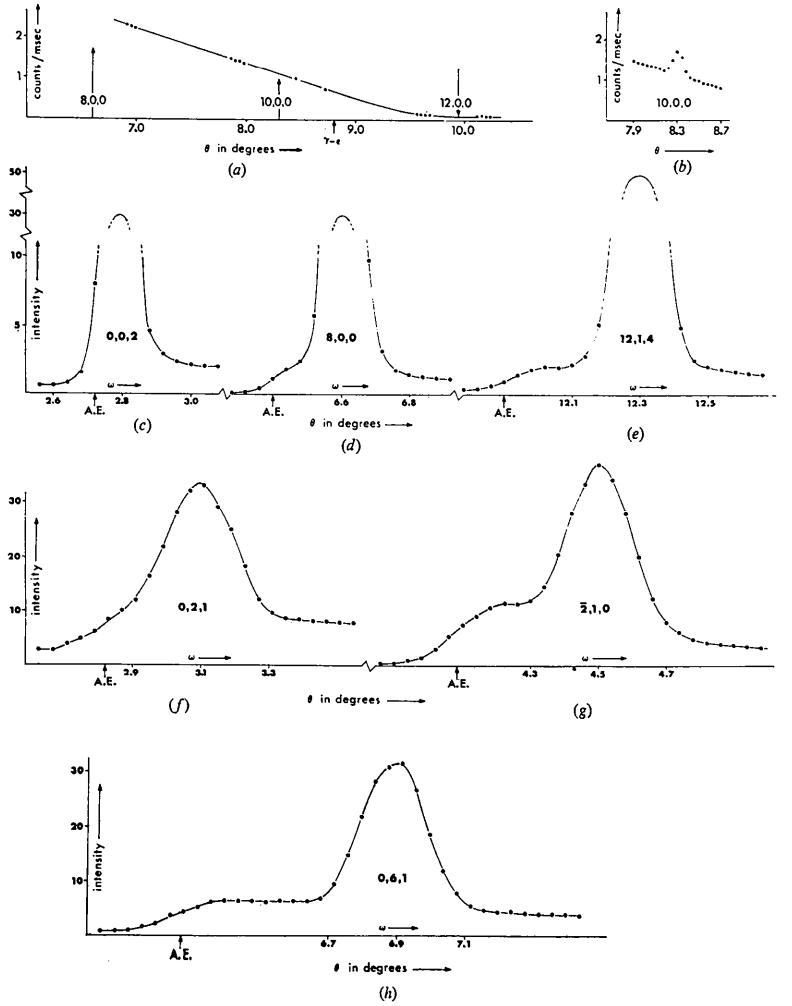

Fig. 5. Some observed reflexion profiles ($\omega/2\theta$ scans on a four-circle diffractometer) from NH_4HSO_4 (AHS) recorded with Zr-filtered Mo $K\alpha$ at an H.T. of 50 kV [(*a*) to (*e*)], and from KD_2PO_4 (DKDP) with Pd-filtered Ag $K\alpha$ at an H.T. of 44 kV [(*f*) to (*h*)]. Pulse-height analysis was used in all cases. (*a*) shows the white-radiation profile on the high-angle side of the 800 reflexion. (*b*) shows the weak 10,0,0 reflexion mounted on this 800 white-radiation profile; the 12,0,0 reflexion is weaker still. Thus the 10,0,0 and 12,0,0 reflexions have a negligible effect on the profile shown in (*a*). The point $\gamma-\epsilon$ is explained in the text. Lp corrections have been applied to the measurements (shown by the dots) and the general background has been removed. Profiles (*c*), (*d*) and (*e*) show the changing form of $I_0(\theta)$ with θ for the AHS measurements. The measured points are separated by 0·04°. The position at which the filter absorption-edge wavelength is reflected is marked A.E. The profiles have been drawn to facilitate comparison of the changing form of the white-radiation profile, $I_b^R(\theta)$, with θ: the intensity scale is arbitrary and is not the same for all three profiles. Diagrams (*f*), (*g*) and (*h*) similarly illustrate the changing form of $I_0(\theta)$ and $I_b^R(\theta)$ with θ for the DKDP measurements.

procedure [see Blessing, Coppens & Becker (1974)]. Other structure in the background (see § 2) and spurious peak shapes will be detected; and counting statistics are improved, particularly for weak reflexions, by excluding background level counts from 'the peak' (which cannot be done in the BPB method, for example).

Some other measures recommend themselves insofar as it is preferable to remove the background by making measurements of the linear part of $I_b^R(\theta)$ on both sides of the characteristic peak. To this end procedures that extend $I_b^R(\theta)$ on the low-angle side of the characteristic wavelength and which decrease the width of I_c^R are desirable. And if the width, 2ϵ, of I_c^R is reduced so also must be the width of the rise at A.E. (see Figs. 3 and 4). $I_b^R(\theta)$ is extended by choosing a filter with an absorption edge close to the $K\beta$ wavelength. On these grounds niobium (Nb) is preferred to Zr as a filter for Mo radiation and Pd is preferred to rhodium (Rh) as a filter for Ag radiation. The width of I_c^R may be decreased by using a small crystal, a small source, and a large source–crystal distance (the effect of crystal imperfection is usually relatively insignificant): there are, of course, other considerations that limit the extent to which these criteria can be pursued. Fig. 5 illustrates these points. The measurements on DKDP [(*f*) to (*h*)] were made with the preferred filter (Pd) for Ag $K\alpha$; the measurements on AHS [(*c*) to (*e*)] were made with the less desirable filter (Zr) for Mo $K\alpha$. It can be seen how the absorption edge moves away from the characteristic peak much more rapidly with θ in the former case. On the other hand the advantage so gained is partly lost because an unusually large specimen was used for the DKDP data collection and the characteristic peak profile, I_c^R, is consequently somewhat broader than in the AHS experiment.

When, in spite of such measures, the situation depicted in Fig. 4(*a*) does arise the procedure adopted makes use of the four principal features (1,2,3 and 4) of $I_b^R(\theta)$ given in the previous section. In Fig. 3 the position of A.E. in the scan, relative to the peak of I_c^R, is determined by the known difference between the $K\bar{\alpha}$ and the filter absorption-edge wavelengths [it is assumed, and found in practice, that the structure of $I_b^R(\theta)$ does not move the peak position of I_c^R significantly]. The values of ε and γ are found from measured profiles as explained in the previous section. The position of ω_p relative to A.E. is then obtained from equation (2). The linear part of $I_b^R(\theta)$ is constructed from the individual step-scan measurements on the high-angle side of I_c^R, and the ordinate P at ω_p is thus determined. Features 1 and 4 of the background profile allow the area under $I_b^R(\theta)$ to the low-angle side of ω_p to be approximated closely by the area under the line AP (Fig. 3). The position of A is determined as being at $\omega=\epsilon$ relative to A.E. Hence the components of the observed reflexion profile, $I_0(\theta)$, can be reconstructed as shown in Fig. 6. Because α to π (see Fig. 6) is nearly 2ϵ the point A lies outside the characteristic peak, I_c^R, on the general background I_g. The most general case considered here for I_g is shown – I_g varying with ω, but linear. The point W is taken at or beyond the high-angle limit of I_c^R. The integrated intensity, I, under I_c^R is then the area under $I_0(\theta)$ integrated from α to Ω minus the area $\alpha APW\Omega$. This simple computation can be done graphically or numerically from the individual step-scan counts. The method will be referred to subsequently as the 'reconstruction method'.

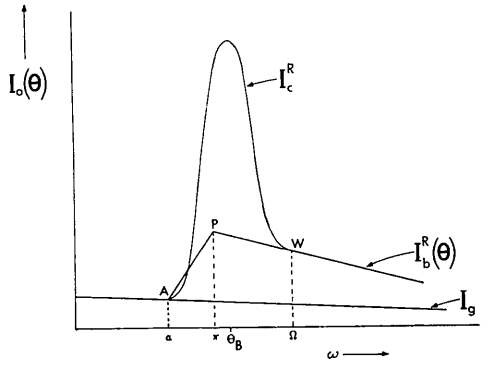

Fig. 6. A reconstruction of the components of $I_0(\theta)$ for the removal of the integrated background intensity contributed by $I_b^R(\theta)$ and I_g. π is equivalent to ω_p.

It has been found in practice that when the reconstruction method is applied 'by hand' adequate corrections are obtained with greatly reduced labour if the technique is applied only to sufficient reflexions to establish a curve of correction factor as a function of θ. (Fig. 7 is an example of this.)

4. Results

The reconstruction and βPB methods have been applied to four-circle diffractometer data collected with Zr-filtered Mo $K\alpha$ data from ammonium hydrogen sulphate (AHS), NH_4HSO_4 (Nelmes, 1969), and chromium chlorine boracite (CCB), $Cr_3B_7O_{13}Cl$ (Nelmes & Thornley, 1974), and with Pd-filtered Ag $K\alpha$ from potassium dideuterium phosphate (DKDP), KD_2PO_4 (Nelmes, 1972; Nelmes & Gould, 1975). In the case of the AHS data the procedures were incorporated into the data-reduction program [see Nelmes (1969) for details]; for CCB and DKDP the procedures were applied graphically.

The AHS data were all collected as step-scan profiles from which the backgrounds were computed as the mean of all the counts beyond the extremities of the characteristic peak (thereby maximizing the precision of I). The BPB method of measurement was used for CCB and DKDP. For both methods the integrated intensities thus obtained were in error ('uncorrected') in the low-θ range; limiting the background measurements to the linear part of $I_b^R(\theta)$ – the βPB method – or, if necessary, applying the reconstruction method yields a 'corrected' value. The uncorrected CCB and DKDP data overestimated low-θ intensities by up to 15 and 100% respectively. The method used to com-

pute the uncorrected AHS intensities is equivalent to a BPB method of smaller angular separation of the background measurements than would generally be used. The overestimation is thus less (up to 6%) than in the case of CCB.

Fig. 7 shows the correction factors required for the DKDP data as a function of θ. The spread is a measure of the maximum uncertainty: some of the spread will be caused by the variation of the characteristic peak position relative to the background measurements in the BPB determination of the uncorrected intensity.

It is clear that the correction is required in principle and that it is significant, particularly in the case of the Ag $K\alpha$ measurements. Where the reconstruction method has to be used it is not possible to assess the accuracy of the corrections fully within single data sets. To do so the corrected intensities should be compared with those obtained by another technique such as careful measurement with monochromated radiation. There is, however, a restricted comparison available: if the reconstruction method is applied to reflexions of the type shown in Fig. 4(*b*) it is found that the integrated intensities obtained agree with those from the direct βPB method to within 2–3%; and as the separation of ω_p from the limit of I_c^R decreases the correction factor yielded by the reconstruction method varies continuously through the transition to the case of Fig. 4(*a*). In Fig. 7 this transition is at $\theta \sim 6°$.

The question remains as to whether the correction affects significantly the results of a crystal-structure refinement. The analysis of DKDP has been carried through with both the corrected and the uncorrected data sets. DKDP is non-centrosymmetric (space group $P2_1$). 3240 independent reflexions were measured out to $\theta = 26°$ with Ag $K\alpha$. The 140 reflexions with $\theta \leq 9°$ were corrected for the effect of structured background. Let the uncorrected data set be denoted *A*, and the corrected set, *B*. Structural parameters were refined for the potassium (K), phosphorus (P) and oxygen (O) atoms. With set *A* only two of the eight independent deuterium atoms could be located; six were found with set *B*. Most of the reflexions with $\theta \leq 9°$ had F_{obs} greater than F_{calc} in set *A*, and so no extinction correction could be applied; with set *B* extinction corrections (on intensity) of up to 50% were required. Table 1 shows the conventional *R* index as a function of θ for the final refinements with both sets. This not only indicates the overall improved fit obtained with the corrected data but suggests that the intensities obtained in the low-angle range ($\leq 9°$) are of an accuracy comparable with that given by BPB measurements at higher angles. The final refinements showed no significant differences in the structural parameters of the K, P and O atoms. But their estimated standard deviations (e.s.d.'s) decreased by about 40% with the corrected data.

A similar comparison made with the CCB Mo $K\alpha$ data, with the 13 lowest-angle reflexions (out of 215) corrected by up to 15% on intensity, showed no significant difference between the values of the two final parameter sets, though the e.s.d.'s fell by about 13%. The *R* index for these 13 reflexions decreased from 3·6 to 2·8% on the introduction of the correction – with an overall *R* index of 2·4%. CCB has a highly symmetric structure (space group $F\bar{4}3c$).

In the light of these two comparative studies and the magnitude of the intensity errors involved it is evident that the decision as to whether or not to make the suggested corrections turns (*a*) on how much any particular experiment depends on the accuracy of low-θ data and (*b*) on how certain the experimenter is of the answer to (*a*) without testing it! The errors are certainly large: but, as seen, they may have little effect on the *values* of refined parameters. As is to be expected the *precision* of the parameters is increased by eliminating the errors.

5. Conclusion

β-filtered radiation is still commonly chosen for the collection of single-crystal X-ray data. The choice may

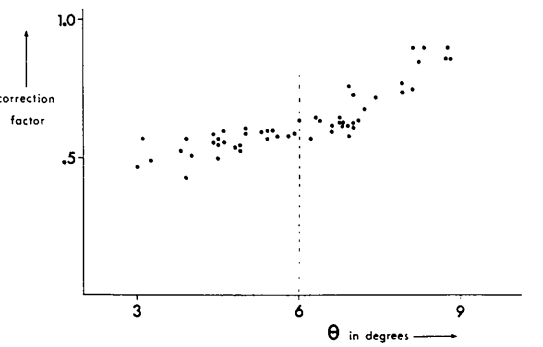

Fig. 7. The correction factors applied to the DKDP intensity data by graphical application of the reconstruction method. The uncorrected data were collected with Pd-filtered Ag $K\alpha$ radiation and the BPB method was used. Below $\theta \sim 6°$ the reconstruction method had to be used; above this value of θ low-angle background measurements were available as in Fig. 4(*b*) – see Fig. 5(*h*) – so that βPB calculations could be made for comparison. The 'best line' drawn through these points was used to correct the intensity of other reflexions in this θ range (see text).

Table 1. *A comparison of R index as a function of θ for the uncorrected data set A, and the equivalent corrected set, B*

$$R \text{ index} = \sum||F_o| - |F_c||/\sum|F_o|.$$

θ range	$\leq 9°$	9–15°	15–19°	19–22°	22–25°	25–27°	0–27° (overall)
R index for *A*	12·7	4·5	5·4	5·8	8·4	11·0	6·8
R index for *B*	3·6	2·5	3·8	5·3	8·1	10·3	4·9

represent the unavailability of more sophisticated techniques or an inertia of methodology: it may equally be the correct conclusion of a careful evaluation of the experiment to be performed.

The main drawbacks of the β-filter method are (i) the difficulty of obtaining precise measurements of weak reflexions in the presence of a relatively high general background, I_g, and (ii) the problem of removing correctly the white-radiation background, $I_b^R(\theta)$. In principle the use of a monochromator overcomes the first of these. But a monochromator gives an incident beam that is generally less intense than the β-filtered beam, and, more importantly, less uniform (in both intensity – *cf.* Fig. 5 of Coppens *et al.* (1974) – and spectral distribution), so that significant errors can arise with non-spherical specimens [see also Young, (1965, 1969)]. The problem of relatively high I_g is not overcome with balanced filters: furthermore, balanced filters not only need to be very well matched but also require about twice the exposure time of the β-filter method to reach a given level of statistical accuracy. The same objections attach to the use of a monochromator or balanced filters to remove $I_b^R(\theta)$. In fact there is a further objection to balanced filters in this context. They do not remove the part of $I_b^R(\theta)$ that is in the region of the characteristic line and the amount of $I_b(\theta)$ included in this region is θ dependent (Cochran, 1950).

The reconstruction method could be improved in principle by a more accurate representation of the white-radiation profile, $I_b(\theta)$, and of the experimental resolution function, R. It would be of interest to compare low-angle data obtained by the β-filter technique – perhaps optimized in this way – with those obtained by careful use of a monochromator and of balanced filters.

To make the routine use of the β-filter technique preferable in practice, it is certainly desirable that the suggested procedures be incorporated into the data-reduction program rather than having to carry them through 'by hand'. Also it is as well not to be faced with the labour of 'by hand' computation when deciding whether an experiment really requires accurate low-angle data, or when choosing between the short-wavelength radiations discussed in this paper and the relatively unaffected Ni-filtered Cu $K\alpha$. An incidental advantage of programming these procedures is that the whole step scan is required (Blessing *et al.*, 1974). It is then relatively simple to include routines to (for example) detect spurious counts, inspect peak shapes and optimize the use of background counts in extracting the integrated intensity.

The principal conclusion of this paper is, then, that the white-radiation background can be removed easily and accurately enough to make the β-filter technique arguably the best choice for most experiments. Monochromator and balanced-filter techniques can be reserved for use only under optimum conditions for the most demanding experiments.

It is reiterated that though the procedures given in this paper have assumed diffractometer data collection they apply *mutatis mutandis* to data collection on film.

Finally it is pointed out that, as indicated by the example in § 4, failure to correct β-filter data for the errors discussed in this paper will contribute to the uncertainties in the physical significance of extinction corrections.

The author would like to thank Dr F. R. Thornley for several helpful discussions, and Dr S.E.B. Gould for her considerable assistance in applying the graphical corrections to the CCB and the DKDP data and in carrying through the various DKDP refinements. The support of a Science Research Council Research Fellowship is gratefully acknowledged.

References

ALEXANDER, L. E. & SMITH, G. S. (1962). *Acta Cryst.* **15**, 983–1004.
BLESSING, R. H., COPPENS, P. & BECKER, P. (1974). *J. Appl. Cryst.* **7**, 488–492.
COCHRAN, W. (1950). *Acta Cryst.* **3**, 268–278.
COPPENS, P., ROSS, F. K., BLESSING, R. H., COOPER, W. F., LARSEN, F. K., LEIPOLDT, J. G., REES, B. & LEONARD, R. (1974). *J. Appl. Cryst.* **7**, 315–319.
KHEIKER, D. M. (1969). *Acta Cryst.* A**25**, 82–88.
LADELL, J. & SPIELBERG, N. (1966). *Acta Cryst.* **21**, 103–118.
NELMES, R. J. (1969). Thesis, University of Edinburgh.
NELMES, R. J. (1972). *Phys. Stat. Sol.* (*b*), **52**, K89–93.
NELMES, R. J. & GOULD, S. E. B. (1975). To be published.
NELMES, R. J. & THORNLEY, F. R. (1974). *J. Phys. C.* **7**, 3855–3874.
YOUNG, R. A. (1965). *Trans. Amer. Cryst. Assoc.* **1**, 42–66.
YOUNG, R. A. (1969). *Acta Cryst.* A**25**, 55–66.